

Optical solitons to Sasa-Satsuma model in birefringent fibers by Laplace-Adomian decomposition method

OSWALDO GONZÁLEZ-GAXIOLA¹, ANJAN BISWAS^{2,3,4,5,6,*}, YAKUP YILDIRIM⁷, ABDULAH A. ALGHAMDI³

¹Applied Mathematics and Systems Department, Universidad Autónoma Metropolitana-Cuajimalpa, Vasco de Quiroga 4871, 05348 Mexico City, Mexico

²Department of Mathematics and Physics, Grambling State University, Grambling, LA-71245, USA

³Mathematical Modeling and Applied Computation (MMAC) Research Group, Department of Mathematics, King Abdulaziz University, Jeddah-21589, Saudi Arabia

⁴Department of Applied Mathematics, National Research Nuclear University, 31 Kashirskoe Hwy, Moscow-115409, Russian Federation

⁵Department of Applied Sciences, Cross-Border Faculty of Humanities, Economics and Engineering, Dunarea de Jos University of Galati, 111 Domneasca Street, Galati-800201, Romania

⁶Department of Mathematics and Applied Mathematics, Sefako Makgatho Health Sciences University, Medunsa-0204, Pretoria, South Africa

⁷Department of Computer Engineering, Biruni University, 34010 Istanbul, Turkey

This paper employs the powerful Laplace-Adomian decomposition scheme to study pulse polarization in birefringent fibers that is governed by Sasa-Satsuma equation is achieved for the first time. Both bright and dark soliton solutions are numerically addressed. The error measure stays impressively controlled by the scheme. The solitons that arise analytically from the governing system are almost identical to the numerical simulations carried out using LADM. The suggested iterative method obtains the solution devoid of any linearization, limiting assumptions, or discretization.

Received February 15, 2022; accepted December 6, 2022)

Keywords: Nonlinear Schrödinger equation; Sasa-Satsuma model; Birefringent fibers; Solitons; Adomian polynomials

1. Introduction

One of the detrimental features of soliton transmission across inter-continental distances is pulse polarization that is referred to as the phenomena of birefringence. This results in the governing model to split into vector-coupled system. This paper studies the split pulse dynamics numerically by Laplace-Adomian decomposition method (LADM). The governing model is the Sasa-Satsuma equation (SSE) that addresses the dynamics of soliton propagation across trans-continental and trans-oceanic distances in presence of perturbation terms which are of Hamiltonian type [1–6]. These perturbative effects stem from third order dispersion, self-steepening effect and nonlinear dispersion. Bright and dark soliton solutions are numerically sketched with the implementation of LADM. The surface plots are compared with the ones that are obtained analytically. The agreement is truly awesome as indicated in the error tables! The details of the scheme along with the error tables of bright and dark solitons are enumerated and exhibited. It should also be clarified that the Sasa-Satsuma equation with the effect of birefringence has recently been studied by other methods, for example, taking account the F -expansion scheme in [2], the modified simple equation approach in [8], and the trial equation approach in [9], but to our knowledge, it has

never yet been solved using the decomposition strategy we suggest.

Our work is divided in several sections. In the section “Governing equation”, we provide a brief introduction to the model given by the Sasa-Satsuma equation, taking the birefringence effect into consideration. In “Formulation of Laplace-Adomian decomposition method and its application” section, describes how to estimate the solution of the Sasa-Satsuma equation in birefringent fibers using the Laplace-Adomian decomposition technique. In the “Numerical Computation” section, the results of numerical experiment are shown in tables and graphs. In the final part, “Conclusions” we synthesize our results and present our conclusive words.

2. Governing model

The Sasa-Satsuma governing model [7] is displayed as follows

$$u_t + au_{xx} + b|u|^2u + i[au_{xxx} + \beta|u|^2u_x + \theta(|u|^2)_xu] = 0. \quad (1)$$

The first term describes the temporal evolution of optical soliton molecules, while the coefficient b describes the Kerr law fiber nonlinearity. In addition, the group velocity dispersion term is given the coefficient a , and the optical

soliton pulse profile is matched by $u(x, t)$. Lastly, the coefficients for self-steepening, stimulated Raman scattering, and third-order dispersion are given by β , θ and α .

The Sasa-Satsuma model in birefringent fibers is given by the system of two coupled one dimensional nonlinear Schrödinger equations in the form [8, 9]

$$\begin{aligned} & i\psi_t + a_1\psi_{xxx} + (b_1|\psi|^2 + c_1|\varphi|^2)\psi \\ & + i[\alpha_1\psi_{xxx} + \gamma_1\varphi_{xxx} + (\beta_1|\psi|^2 + \eta_1|\varphi|^2)\psi_x \\ & + (\theta_1(|\psi|^2)_x + \lambda_1(|\varphi|^2)_x)\psi] = 0, \end{aligned} \quad (2)$$

$$\begin{aligned} & i\varphi_t + a_2\varphi_{xxx} + (b_2|\varphi|^2 + c_2|\psi|^2)\varphi \\ & + i[\alpha_2\varphi_{xxx} + \gamma_2\psi_{xxx} + (\beta_2|\varphi|^2 + \eta_2|\psi|^2)\varphi_x \\ & + (\theta_2(|\varphi|^2)_x + \lambda_2(|\psi|^2)_x)\varphi] = 0, \end{aligned} \quad (3)$$

with the inclusion of the self-steepening, stimulated Raman scattering in additionally third-order dispersion that sequentially are given with the real coefficients β_j , η_j , θ_j , λ_j , α_j and γ_j . Moreover ψ and φ are the complex amplitudes or envelopes of the two wave packets, respectively. It must be noted that in order to derive (2) and (3) from (1), for birefringent fibers, it is necessary to split $u(x, t) = \psi(x, t) + \varphi(x, t)$ and substitute into (1) and then write the two components of the equation after neglecting the effects of four wave mixing.

Several mathematical models including coupled nonlinear Schrödinger equations are related to the current research. Further details are in [10-13] and references therein.

2.1. Bright solitons

In order to look for bright solitons to the nonlinear Sasa-Satsuma equation having two different refractive indices given by (2-3), the starting points are [8]:

$$\psi(x, t) = A_1 \operatorname{sech}[B_1(x - vt)]e^{i[-\kappa x + \omega t + \theta]}, \quad (4)$$

$$\varphi(x, t) = A_2 \operatorname{sech}[B_2(x - vt)]e^{i[-\kappa x + \omega t + \theta]}, \quad (5)$$

where, the amplitudes for every $j = 1, 2$, are given by

$$A_j = \sqrt{\frac{2(\kappa^3\alpha_j + \kappa^3\gamma_j + \kappa^2a_j + \omega)}{\kappa\beta_j + \kappa\eta_j + b_j + c_j}}, \quad (6)$$

and the inverse width of the solitons B_j are obtained as

$$B_j = \sqrt{\frac{\kappa^3\alpha_j + \kappa^3\gamma_j + \kappa^2a_j + \omega}{3\kappa\alpha_j + 3\kappa\gamma_j + a_j}}. \quad (7)$$

Moreover, the soliton speed, the frequency, the angular velocity and the phase center are ensured by the coefficient of v , κ , ω , θ respectively. Particularly, for the bright solitons to exist, the conditions

$$\begin{aligned} & (\kappa\beta_j + \kappa\eta_j + b_j + c_j) \\ & \times (\kappa^3\alpha_j + \kappa^3\gamma_j + \kappa^2a_j + \omega) > 0, \end{aligned} \quad (8)$$

$$\begin{aligned} & (3\kappa\alpha_j + 3\kappa\gamma_j + a_j) \\ & \times (\kappa^3\alpha_j + \kappa^3\gamma_j + \kappa^2a_j + \omega) > 0, \end{aligned} \quad (9)$$

must be fulfilled.

2.2. Dark solitons

In order to look for dark solitons to the nonlinear Sasa-Satsuma equation having two different refractive indices given by (2-3), the starting points are [8]:

$$\psi(x, t) = C_1 \tanh[D_1(x - vt)]e^{i[-\kappa x + \omega t + \theta]}, \quad (10)$$

$$\varphi(x, t) = C_2 \tanh[D_2(x - vt)]e^{i[-\kappa x + \omega t + \theta]}, \quad (11)$$

where, the amplitudes for every $j = 1, 2$, are given by

$$C_j = \sqrt{\frac{\kappa^3\alpha_j + \kappa^3\gamma_j + \kappa^2a_j + \omega}{\kappa\beta_j + \kappa\eta_j + b_j + c_j}}, \quad (12)$$

and the inverse width of the solitons B_j are obtained as

$$D_j = \sqrt{-\frac{\kappa^3\alpha_j + \kappa^3\gamma_j + \kappa^2a_j + \omega}{2(3\kappa\alpha_j + 3\kappa\gamma_j + a_j)}}. \quad (13)$$

Moreover, the soliton speed, the frequency, the angular velocity and the phase center are ensured by the coefficient of v , κ , ω , θ respectively. Specifically, for the dark solitons to exist, the conditions

$$\begin{aligned} & (\kappa\beta_j + \kappa\eta_j + b_j + c_j) \\ & \times (\kappa^3\alpha_j + \kappa^3\gamma_j + \kappa^2a_j + \omega) > 0, \end{aligned} \quad (14)$$

$$\begin{aligned} & (3\kappa\alpha_j + 3\kappa\gamma_j + a_j) \\ & \times (\kappa^3\alpha_j + \kappa^3\gamma_j + \kappa^2a_j + \omega) < 0, \end{aligned} \quad (15)$$

must be fulfilled.

3. Formulation of Laplace-Adomian decomposition method and its application

In this section, we present a Laplace Adomian decomposition method (LADM) for obtaining a solution of nonlinear partial differential equations. The method was originally established in the mid-1980s by G. Adomian and R. Rach in [14], and its applications today are numerous. We will also apply the algorithm provided by the method to solve the Sasa-Satsuma in birefringent fibers model given by equations (2) and (3).

3.1. The general algorithm provided by LADM

To show the basic idea of LADM, we consider the following PDE in general operator form

$$L_t u(x, t) + Ru(x, t) + Nu(x, t) = 0. \quad (16)$$

where L_t is the linear derivative operator in t , R is the highest order linear derivative operator in x and N is the nonlinear term. In addition, the PDE will be subject to the initial condition:

$$u(x, 0) = f(x). \quad (17)$$

If the Laplace transform \mathcal{L} with respect to t is applied to both sides of the Eq. (16) and considering the initial condition, it becomes,

$$su(x, s) - u(x, 0) = \mathcal{L}\{Ru(x, t) + Nu(x, t)\}. \quad (18)$$

If the Eq. (18) is simplified is simplified using \mathcal{L}^{-1} we obtain

$$u(x, t) = f(x) + \mathcal{L}^{-1}\left[\frac{1}{s}\mathcal{L}\{Ru(x, t) + Nu(x, t)\}\right]. \quad (19)$$

The solution $u(x, t)$ is given by

$$u(x, t) = \sum_{n=0}^{\infty} u_n(x, t), \quad (20)$$

and the non-linear term, is represented by Adomain polynomials

$$Nu(x, t) = \sum_{n=0}^{\infty} A_n(u_0, u_1, \dots, u_n), \quad (21)$$

where the Adomian polynomials in the case of a variable are defined as [15, 16]

$$A_0 = N(u_0),$$

$$A_n = \frac{1}{n} \sum_{k=0}^{n-1} (k+1) u_{k+1} \frac{\partial}{\partial u_k} A_{n-1}, \quad n \geq 1. \quad (22)$$

Using Eqs. (20) and (21) in Eq. (19), we obtain

$$\begin{aligned} \sum_{n=0}^{\infty} u_n(x, t) &= f(x) \\ &+ \mathcal{L}^{-1}\left[\frac{1}{s}\mathcal{L}\left\{R\left(\sum_{n=0}^{\infty} u_n(x, t)\right)\right.\right. \\ &\left.\left.+ \sum_{n=0}^{\infty} A_n(u_0, u_1, \dots, u_n)\right\}\right]. \end{aligned} \quad (23)$$

Matching terms on the both sides, we acquire

$$u_0(x, t) = f(x),$$

$$u_1(x, t) = \mathcal{L}^{-1}\left[\frac{1}{s}\mathcal{L}\{Ru_0(x, t) + A_0(u_0)\}\right],$$

$$u_2(x, t) = \mathcal{L}^{-1}\left[\frac{1}{s}\mathcal{L}\{Ru_1(x, t) + A_1(u_0, u_1)\}\right],$$

⋮

$$\begin{aligned} u_n(x, t) &= \mathcal{L}^{-1}\left[\frac{1}{s}\mathcal{L}\{Ru_{n-1}(x, t)\right. \\ &\left.+ A_{n-1}(u_0, u_1, \dots, u_{n-1})\right]. \end{aligned}$$

In this way computing direct and inverse Laplace transform we get the approximate solution in the form of finite sum as

$$\begin{aligned} u(x, t) &= u_0(x, t) + u_1(x, t) \\ &+ u_2(x, t) + \dots + u_N(x, t). \end{aligned} \quad (24)$$

It is important to mention that u_0 is the first approximation that satisfies the boundary condition. In the next subsection, we will implement the recursive algorithm generated throughly LADM for the solution of the nonlinear Sasa-Satsuma in birefringent fibers model. The algorithm described above has been successfully applied in similar problems, which we can see in [17].

3.2. The method implementation for Sasa-Satsuma equation

Consider the Sasa-Satsuma model represented by (2) and (3). In order to obtain analytical approximate solutions for (2) and (3) using LADM, we first rewrite the equation in the following operator form:

$$\begin{aligned} D_t \psi &= ia_1 L_{2x} \psi + i(b_1 |\psi|^2 + c_1 |\varphi|^2) \psi \\ &- [\alpha_1 L_{3x} \psi + \gamma_1 L_{3x} \varphi + ((\beta_1 |\psi|^2 + \eta_1 |\varphi|^2) L_{1x} \psi \\ &+ (\theta_1 L_{1x} (|\psi|^2) + \lambda_1 L_{1x} (|\varphi|^2)) \psi], \end{aligned} \quad (25)$$

$$\begin{aligned} D_t \varphi &= ia_2 L_{2x} \varphi + i(b_2 |\varphi|^2 + c_2 |\psi|^2) \varphi \\ &- [\alpha_2 L_{3x} \varphi + \gamma_2 L_{3x} \psi + (\beta_2 |\varphi|^2 + \eta_2 |\psi|^2) L_{1x} \varphi \\ &+ (\theta_2 L_{1x} (|\varphi|^2) + \lambda_2 L_{1x} (|\psi|^2)) \varphi]. \end{aligned} \quad (26)$$

where $L_{nx} = \frac{\partial^n}{\partial x^n}$ and D_t is the time derivative. The LADM method begins by applying the Laplace transform to (25)-(26), and then, by using given initial conditions, we obtain

$$\psi_0(x, t) = f(x),$$

$$\varphi_0(x, t) = g(x),$$

$$\psi_1(x, t) = \mathcal{L}^{-1}\left[\frac{1}{s}\mathcal{L}\{R_1(\psi_0, \varphi_0) + A_0(\psi_0, \varphi_0)\}\right],$$

$$\varphi_1(x, t) = \mathcal{L}^{-1}\left[\frac{1}{s}\mathcal{L}\{R_2(\psi_0, \varphi_0) + B_0(\psi_0, \varphi_0)\}\right],$$

$$\begin{aligned} \psi_{n+1}(x, t) &= \mathcal{L}^{-1}\left[\frac{1}{s}\mathcal{L}\{R_1(\psi_n, \varphi_n)\right. \\ &\quad \left.+ A_n(\psi_0, \varphi_0, \dots, \psi_n, \varphi_n)\right], \\ \varphi_{n+1}(x, t) &= \mathcal{L}^{-1}\left[\frac{1}{s}\mathcal{L}\{R_2(\psi_n, \varphi_n)\right. \\ &\quad \left.+ B_n(\psi_0, \varphi_0, \dots, \psi_n, \varphi_n)\right]. \end{aligned} \tag{27}$$

In the LADM, the solutions $\psi(x, t)$ and $\varphi(x, t)$ are defined by the infinite series as

$$\begin{aligned} \psi(x, t) &= \sum_{n=0}^{\infty} \psi_n(x, t), \\ \varphi(x, t) &= \sum_{n=0}^{\infty} \varphi_n(x, t). \end{aligned} \tag{28}$$

The nonlinear terms

$$\begin{aligned} N_1(\psi, \varphi) &= i(b_1|\psi|^2 + c_1|\varphi|^2)\psi - ((\beta_1|\psi|^2 \\ &\quad + \eta_1|\varphi|^2)L_{1x}\psi + (\theta_1L_{1x}(|\psi|^2) + \lambda_1L_{1x}(|\varphi|^2))\psi, \end{aligned} \tag{29}$$

$$\begin{aligned} N_2(\psi, \varphi) &= i(b_2|\varphi|^2 + c_2|\psi|^2)\varphi - (\beta_2|\varphi|^2 \\ &\quad + \eta_2|\psi|^2)L_{1x}\varphi + (\theta_2L_{1x}(|\varphi|^2) + \lambda_2L_{1x}(|\psi|^2))\varphi, \end{aligned} \tag{30}$$

are expressed as an infinite series of the Adomian polynomials as

$$\begin{aligned} N_1(\psi, \varphi) &= \sum_{n=0}^{\infty} A_n(\psi_0, \varphi_0, \dots, \psi_n, \varphi_n), \\ N_2(\psi, \varphi) &= \sum_{n=0}^{\infty} B_n(\psi_0, \varphi_0, \dots, \psi_n, \varphi_n), \end{aligned} \tag{31}$$

where the Adomian polynomials A_n and B_m depend on $\psi_0, \dots, \psi_n, \varphi_0, \dots, \varphi_n$ which can be determined by the algorithm defined in [16]:

$$\begin{aligned} A_n &= \frac{1}{n} \left[\sum_{k=0}^{n-1} (k+1)\psi_{k+1} \frac{\partial}{\partial \psi_k} A_{n-1} \right. \\ &\quad \left. + \sum_{k=0}^{n-1} (k+1)\varphi_{k+1} \frac{\partial}{\partial \varphi_k} A_{n-1} \right], n \geq 1, \end{aligned} \tag{32}$$

$$\begin{aligned} B_m &= \frac{1}{m} \left[\sum_{k=0}^{m-1} (k+1)\psi_{k+1} \frac{\partial}{\partial \psi_k} B_{m-1} \right. \\ &\quad \left. + \sum_{k=0}^{m-1} (k+1)\varphi_{k+1} \frac{\partial}{\partial \varphi_k} B_{m-1} \right], m \geq 1. \end{aligned} \tag{33}$$

By applying the algorithm we obtain

$$A_0 = N_1(\psi_0, \varphi_0),$$

$$\begin{aligned} A_1 &= \psi_1 \frac{\partial N_1}{\partial \psi_0}(\psi_0, \varphi_0) + \varphi_1 \frac{\partial N_1}{\partial \varphi_0}(\psi_0, \varphi_0), \\ A_2 &= \psi_2 \frac{\partial N_1}{\partial \psi_1}(\psi_0, \varphi_0) + \varphi_2 \frac{\partial N_1}{\partial \varphi_1}(\psi_0, \varphi_0) \\ &\quad + \frac{1}{2!} \psi_1^2 \frac{\partial^2 N_1}{\partial \psi_1^2}(\psi_0, \varphi_0) + \frac{1}{2!} \varphi_1^2 \frac{\partial^2 N_1}{\partial \varphi_1^2}(\psi_0, \varphi_0) \\ &\quad + \psi_1 \varphi_1 \frac{\partial^2 N_1}{\partial \psi_1 \varphi_1}(\psi_0, \varphi_0), \\ A_3 &= \psi_3 \frac{\partial N_1}{\partial \psi_1}(\psi_0, \varphi_0) + \varphi_3 \frac{\partial N_1}{\partial \varphi_1}(\psi_0, \varphi_0) \\ &\quad + \psi_1 \psi_2 \frac{\partial^2 N_1}{\partial \psi_1^2}(\psi_0, \varphi_0) + \varphi_1 \varphi_2 \frac{\partial^2 N_1}{\partial \varphi_1^2}(\psi_0, \varphi_0) \\ &\quad + \psi_1 \varphi_1 \frac{\partial^2 N_1}{\partial \psi_1 \varphi_1}(\psi_0, \varphi_0) + \psi_1 \varphi_2 \frac{\partial^2 N_1}{\partial \varphi_1 \psi_2}(\psi_0, \varphi_0) \\ &\quad + \frac{1}{2!} \psi_1^2 \varphi_1 \frac{\partial^2 N_1}{\partial \psi_1^2 \psi_2}(\psi_0, \varphi_0) + \frac{1}{2!} \varphi_2^2 \psi_1 \frac{\partial^2 N_1}{\partial \psi_1 \varphi_2^2}(\psi_0, \varphi_0) \\ &\quad + \frac{1}{3!} \psi_1^3 \frac{\partial^3 N_1}{\partial \psi_1^3}(\psi_0, \varphi_0) + \frac{1}{3!} \varphi_1^3 \frac{\partial^3 N_1}{\partial \varphi_1^3}(\psi_0, \varphi_0), \\ B_0 &= N_2(\psi_0, \varphi_0), \\ B_1 &= \psi_1 \frac{\partial N_2}{\partial \psi_0}(\psi_0, \varphi_0) + \varphi_1 \frac{\partial N_2}{\partial \varphi_0}(\psi_0, \varphi_0), \\ B_2 &= \psi_2 \frac{\partial N_2}{\partial \psi_1}(\psi_0, \varphi_0) + \varphi_2 \frac{\partial N_2}{\partial \varphi_1}(\psi_0, \varphi_0) \\ &\quad + \frac{1}{2!} \psi_1^2 \frac{\partial^2 N_2}{\partial \psi_1^2}(\psi_0, \varphi_0) + \frac{1}{2!} \varphi_1^2 \frac{\partial^2 N_2}{\partial \varphi_1^2}(\psi_0, \varphi_0) \\ &\quad + \psi_1 \varphi_1 \frac{\partial^2 N_2}{\partial \psi_1 \varphi_1}(\psi_0, \varphi_0), \\ B_3 &= \psi_3 \frac{\partial N_2}{\partial \psi_1}(\psi_0, \varphi_0) + \varphi_3 \frac{\partial N_2}{\partial \varphi_1}(\psi_0, \varphi_0) \\ &\quad + \psi_1 \psi_2 \frac{\partial^2 N_2}{\partial \psi_1^2}(\psi_0, \varphi_0) + \varphi_1 \varphi_2 \frac{\partial^2 N_2}{\partial \varphi_1^2}(\psi_0, \varphi_0) \\ &\quad + \psi_1 \varphi_1 \frac{\partial^2 N_2}{\partial \psi_1 \varphi_1}(\psi_0, \varphi_0) + \psi_1 \varphi_2 \frac{\partial^2 N_2}{\partial \varphi_1 \psi_2}(\psi_0, \varphi_0) \\ &\quad + \frac{1}{2!} \psi_1^2 \varphi_1 \frac{\partial^2 N_2}{\partial \psi_1^2 \psi_2}(\psi_0, \varphi_0) + \frac{1}{2!} \varphi_2^2 \psi_1 \frac{\partial^2 N_2}{\partial \psi_1 \varphi_2^2}(\psi_0, \varphi_0) \\ &\quad + \frac{1}{3!} \psi_1^3 \frac{\partial^3 N_2}{\partial \psi_1^3}(\psi_0, \varphi_0) + \frac{1}{3!} \varphi_1^3 \frac{\partial^3 N_2}{\partial \varphi_1^3}(\psi_0, \varphi_0), \end{aligned}$$

The analysis introduced above will be illustrated by discussing the following numerical examples in the next section.

4. Numerical computation

We will illustrate the LADM method to find soliton solutions for the Sasa-Satsuma equation for both the bright and dark cases with different coefficient systems. The examples considered below will be solved using *Mathematica* software for the implementation of the algorithm.

4.1. Simulation to bright solitons

We consider the coupled nonlinear SSE equation in birefringent fibers given by the system of Eqs. (2) and (3) and we choose the initial condition:

$$\psi(x, 0) = A_1 \operatorname{sech}[B_1(x)] e^{i[-\kappa x + \theta]}, \quad (34)$$

$$\varphi(x, 0) = A_2 \operatorname{sech}[B_2(x)] e^{i[-\kappa x + \theta]}. \quad (35)$$

Table 1. Bright solitons with SSE, simulations with $N = 14$

Cases	Parameters												Error in φ											
	a_1	a_2	b_1	b_2	c_1	c_2	α_1	α_2	γ_1	γ_2	β_1	β_2		η_1	η_2	θ_1	θ_2	λ_1	λ_2	A_1	A_2	B_1	B_2	Error in ψ
(a)	1.2	1.5	1.8	2.4	1.6	1.1	0.1	0.2	4.1	6.5	2.2	2.5	8.6	7.8	0.9	0.5	0.1	0.7	0.9	1.0	2.4	3.1	1.1 × 10 ⁻⁷	1.8 × 10 ⁻⁷
(b)	1.0	1.4	0.6	0.5	0.9	0.2	0.9	0.6	6.6	4.9	1.6	1.5	9.6	9.0	0.1	0.9	0.8	0.2	1.3	1.4	3.2	2.7	5.5 × 10 ⁻⁸	7.8 × 10 ⁻⁸
(c)	1.2	1.6	-2.0	-2.2	3.6	2.5	5.0	3.1	5.6	2.8	-0.6	-0.1	5.6	3.9	3.6	2.2	1.1	1.1	1.1	1.1	4.0	4.7	6.0 × 10 ⁻⁸	4.8 × 10 ⁻⁸

Table 2. Dark solitons with SSE, simulations with $N = 14$

Cases	Parameters												Error in φ											
	a_1	a_2	b_1	b_2	c_1	c_2	α_1	α_2	γ_1	γ_2	β_1	β_2		η_1	η_2	θ_1	θ_2	λ_1	λ_2	A_1	A_2	B_1	B_2	Error in ψ
(d)	0.2	0.8	1.9	1.7	7.1	6.5	2.1	3.0	0.1	0.3	1.1	0.8	0.3	1.1	9.1	8.2	0.9	1.1	1.3	0.9	3.2	5.1	3.2 × 10 ⁻⁸	2.4 × 10 ⁻⁸
(e)	-0.9	-1.1	0.9	0.1	-1.9	-1.4	6.6	7.1	9.9	6.9	0.9	1.1	0.6	1.3	8.8	9.0	7.0	6.5	0.8	1.3	4.4	4.8	1.8 × 10 ⁻⁸	5.5 × 10 ⁻⁸
(f)	0.2	1.1	9.0	8.2	6.9	4.2	1.1	1.4	7.9	6.6	8.0	6.9	8.4	7.8	-0.6	-0.2	6.1	7.7	1.1	0.9	3.8	4.9	3.1 × 10 ⁻⁸	4.6 × 10 ⁻⁸

The coefficient systems and parameters for these simulations are given in Table 1 and the results are shown in Figs. 1, 2 and 3.

4.2. Simulation to dark solitons

We consider the coupled nonlinear SSE equation in birefringent fibers given by the system of Eqs. (2) and (3) and we choose the initial condition:

$$\psi(x, 0) = C_1 \operatorname{tanh}[D_1(x)] e^{i[-\kappa x + \theta]}, \quad (36)$$

$$\varphi(x, 0) = C_2 \operatorname{tanh}[D_2(x)] e^{i[-\kappa x + \theta]}. \quad (37)$$

The coefficient systems and parameters for these simulations are given in Table 2 and the results are shown in Figs. 4, 5 and 6.

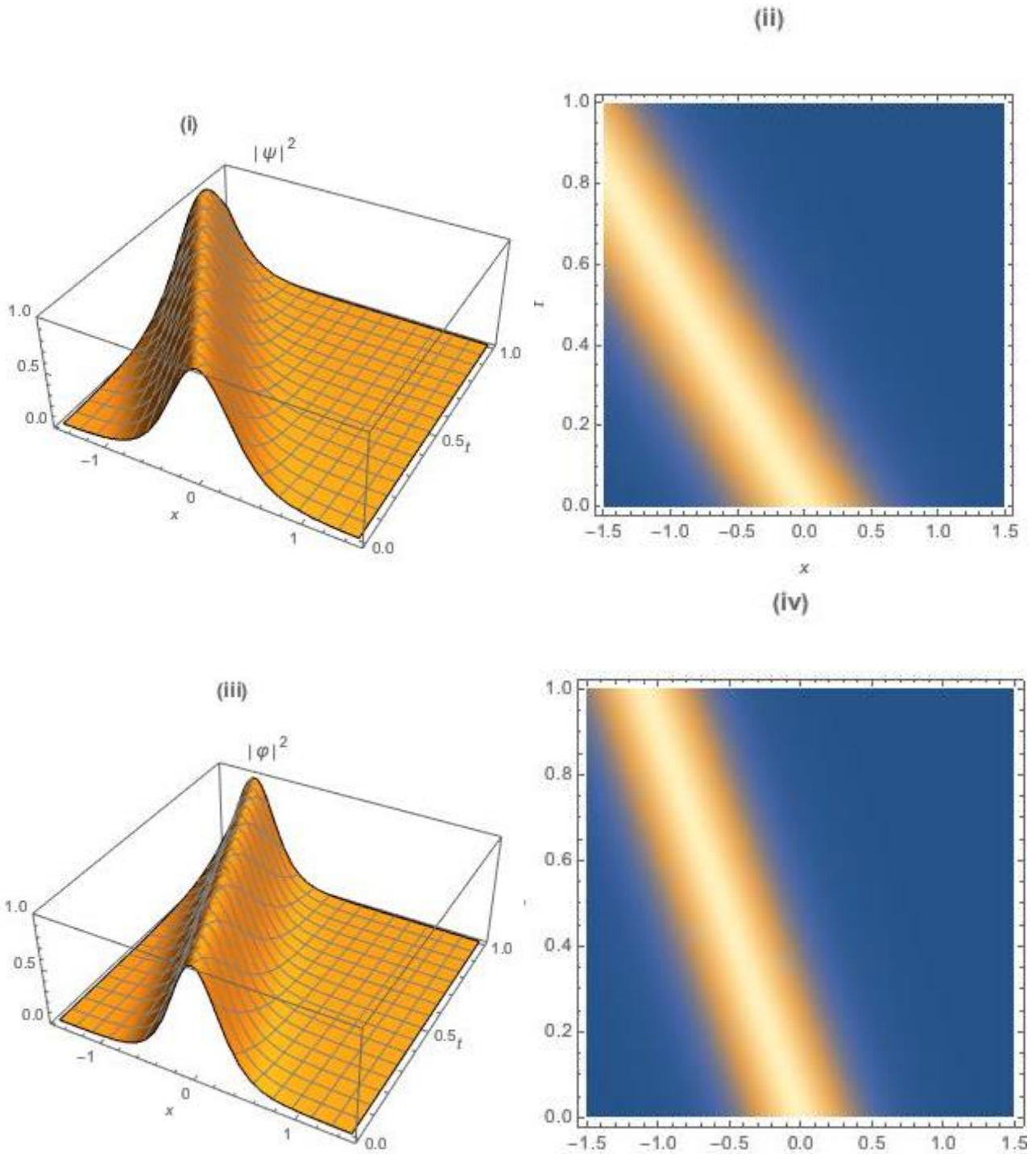


Fig. 1. The numerical simulations of the solutions of the equations (2) and (3) for case (a) of Table 1 with $N = 14$. The dynamic behavior of $|\psi(x,t)|^2$ (i) and corresponding density plot (ii). The dynamic behavior of $|\varphi(x,t)|^2$ (iii) and corresponding density plot (iv) (color online)

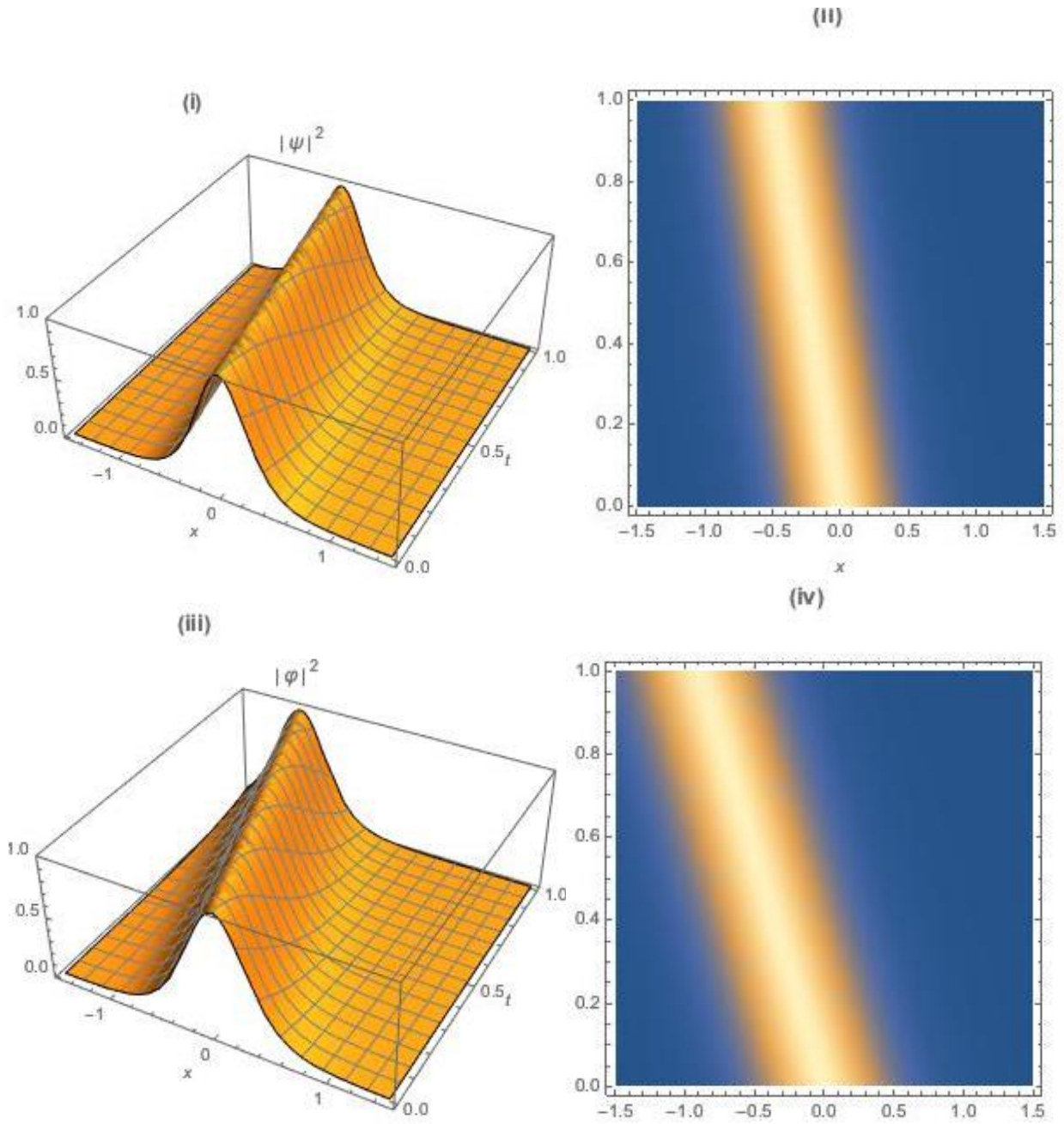


Fig. 2. The numerical simulations of the solutions of the equations (2) and (3) for case (b) of Table 1 with $N = 14$. The dynamic behavior of $|\psi(x, t)|^2$ (i) and corresponding density plot (ii). The dynamic behavior of $|\varphi(x, t)|^2$ (iii) and corresponding density plot (iv) (color online)

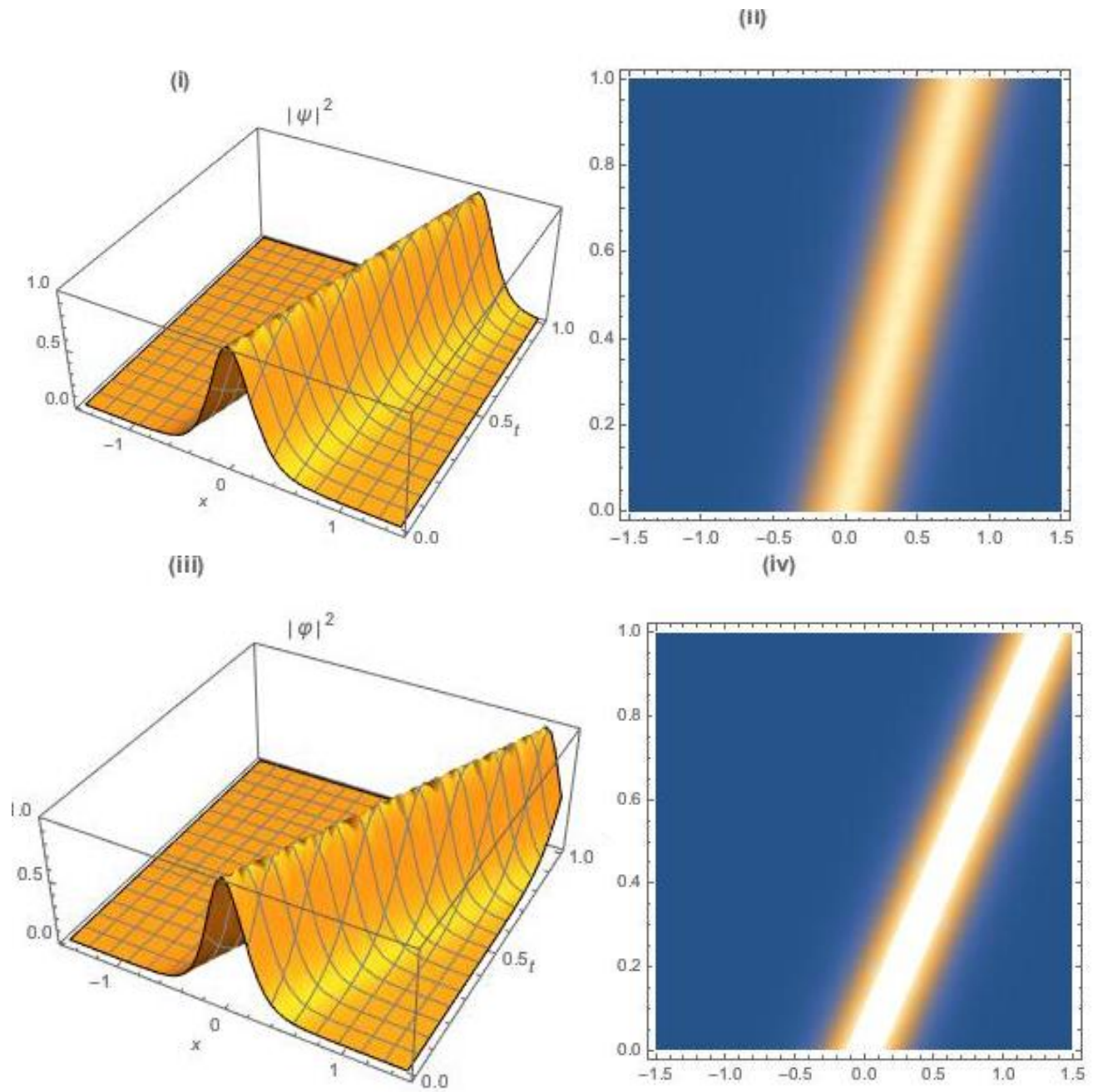


Fig. 3. The numerical simulations of the solutions of the equations (2) and (3) for case (c) of Table 1 with $N = 14$. The dynamic behavior of $|\psi(x, t)|^2$ (i) and corresponding density plot (ii). The dynamic behavior of $|\varphi(x, t)|^2$ (iii) and corresponding density plot (iv) (color online)

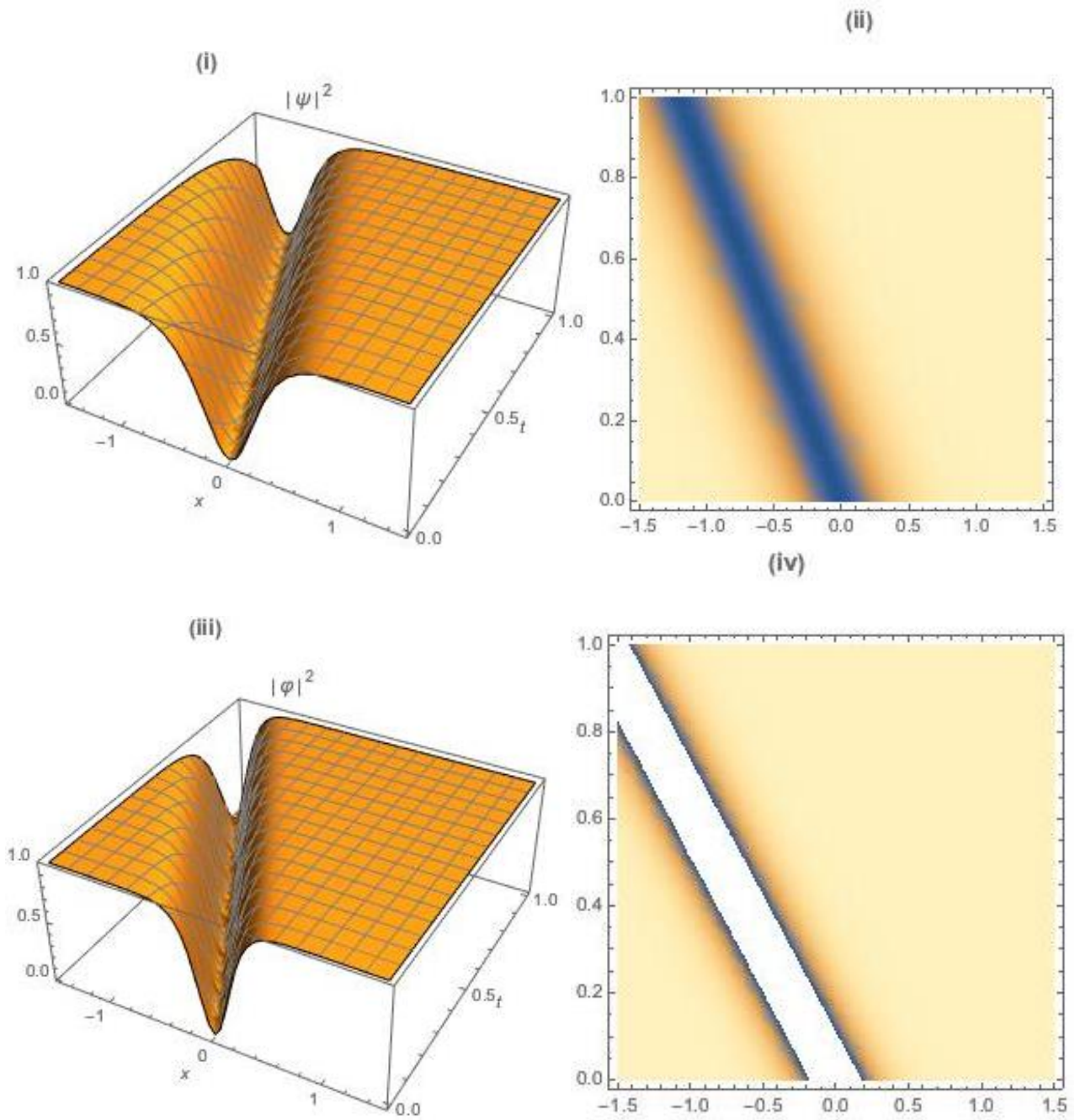


Fig. 4. The numerical simulations of the solutions of the equations (2) and (3) for case (d) of Table 2 with $N = 14$. The dynamic behavior of $|\psi(x, t)|^2$ (i) and corresponding density plot (ii). The dynamic behavior of $|\varphi(x, t)|^2$ (iii) and corresponding density plot (iv) (color online)

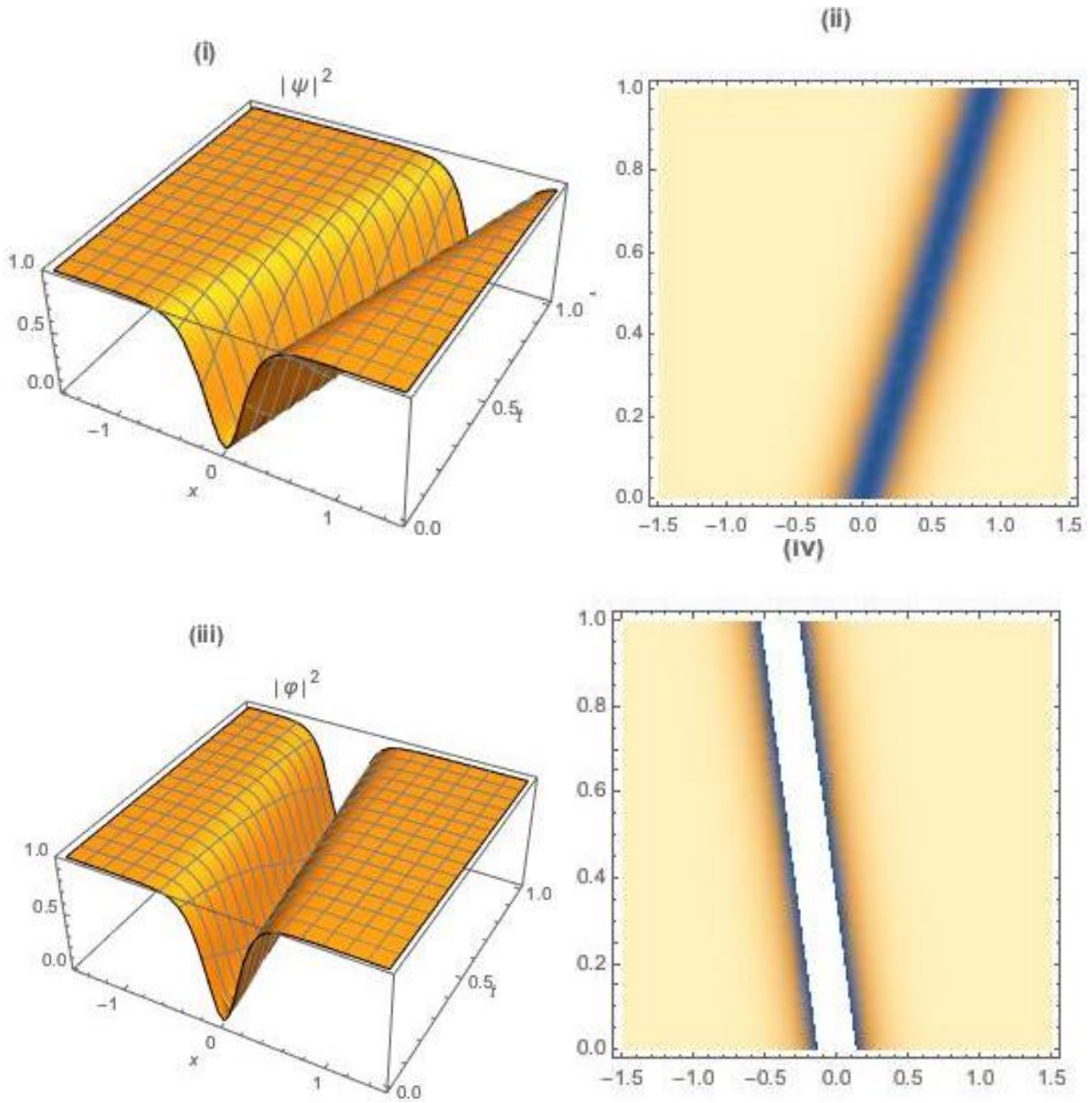


Fig. 5. The numerical simulations of the solutions of the equations (1) and (2) for case (e) of Table 2 with $N = 14$. The dynamic behavior of $|\psi(x, t)|^2$ (i) and corresponding density plot (ii). The dynamic behavior of $|\phi(x, t)|^2$ (iii) and corresponding density plot (iv) (color online)

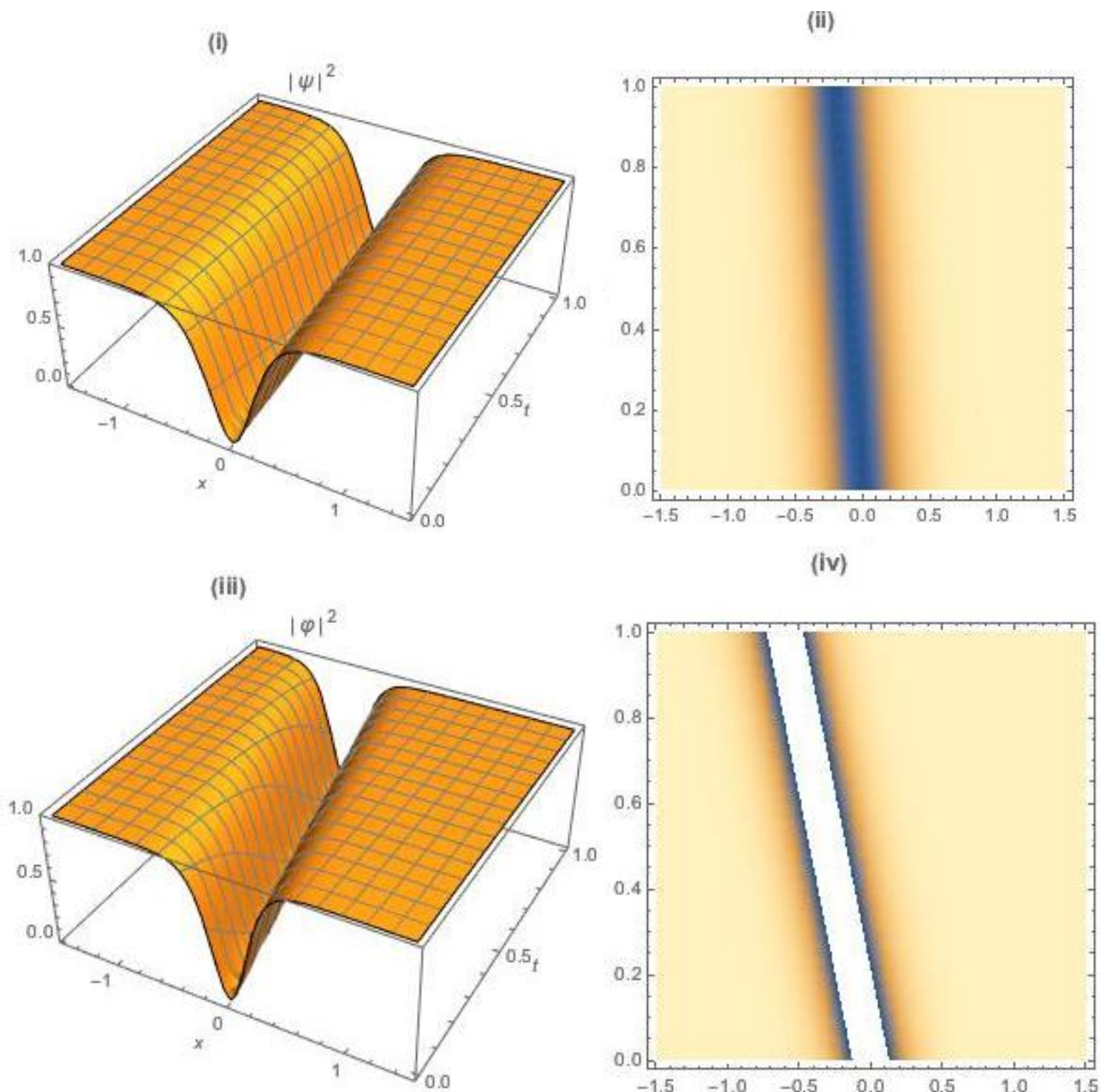


Fig. 6. The numerical simulations of the solutions of the equations (1) and (2) for case (f) of Table 2 with $N = 14$. The dynamic behavior of $|\psi(x, t)|^2$ (i) and corresponding density plot (ii). The dynamic behavior of $|\varphi(x, t)|^2$ (iii) and corresponding density plot (iv) (color online)

In the six examples shown above, the greatest error was on the order of 10^{-7} , indicating that LADM takes less computing effort than traditional techniques. Other advantages include the ability to solve nonlinear problems without linearization, the wide applicability to several types of problems and scientific fields, and the development of a reliable, analytic solution.

5. Conclusions

This paper studied the SSE numerically to visualize bright and dark optical solitons in birefringent fibers. ADM has made this transparency possible. The

perturbation terms are of Hamiltonian type as in the model that is considered for polarization-preserving fibers. The surface plots and error tables are all included. The results are thus a complete display of the numerical analysis of vector-coupled SSE that studies soliton propagation through birefringent fibers. The impressive results thus open up additional avenues to venture SSE numerically that would also yield such surface plots. Some such algorithms are variational iteration approach, finite element method, finite difference scheme and several different approaches. The results of those research undertakings are soon going to be disseminated across the board that will be along the lines of the previously reported results [14-17].

References

- [1] N. Sasa, J. Satsuma, *J. Phys. Soc. Japan* **60**, 409 (1991).
- [2] A. R. Seadawy, A. H. Arnous, A. Biswas, M. R. Belic, *Optoelectron. Adv. Mat.* **13**(1-2), 31 (2019).
- [3] Y. Yildirim, A. Biswas, M. Asma, M. Ekici, H. Triki, E. M. E. Zayed, A. K. Alzahrani, M. R. Belic, *Optik* **219**, 165183 (2020).
- [4] A. R. Adem, B. P. Ntsime, A. Biswas, M. Asma, M. Ekici, S. P. Moshokoa, A. K. Alzahrani, M. R. Belic, *Phys. Lett. A* **384**(27), 126721 (2020).
- [5] C. Li, L. Chen, G. Li, *Optik* **224**, 165527 (2020).
- [6] K. Hosseini, M. Mirzazadeh, J. F. Gómez-Aguilar, *Optik* **224**, 165425 (2020).
- [7] C. Gilson, J. Hietarinta, J. Nimmo, Y. Ohta, *Phys. Rev. E* **68** (1), 016614, (2003).
- [8] Y. Yildirim, *Optik* **184**, 197 (2019).
- [9] Y. Yildirim, *Optik* **185**, 269 (2019).
- [10] W.-P. Zhong, R. Belic, *Phys. Rev. E* **82**, 047601 (2010).
- [11] W.-P. Zhong, R. Belic, *Ann. Phys.* **351**, 787 (2014).
- [12] W.-P. Zhong, R. Belic, B. A. Malomed, *Phys. Rev. E* **92**, 053201 (2015).
- [13] Z. Yang, W.-P. Zhong, W. Zhong, M. R. Belic, *Optik* **193**, 163029 (2019).
- [14] G. Adomian, R. Rach, *J. Math. Anal. Appl.* **114**, 171 (1986).
- [15] A. M. Wazwaz, *Appl. Math. Comput.* **111**(1), 33 (2000).
- [16] J. S. Duan, *Appl. Math. Comput.* **217**(13), 6337 (2011).
- [17] O. González-Gaxiola, A. Biswas, F. Mallawi, M. R. Belic, *J. Adv. Res.* **21**, 161 (2020).

*Corresponding author: biswas.anjan@gmail.com